# Exceptional anticancer photodynamic properties of [1,4-Bis(3,6,9,12-Tetraoxatridec-1-yloxy)phthalocyaninato]zinc(II)

Christophe Nguyen, Isabelle Toubia, Kamel Hadj-Kaddour, Lamiaa M.A. Ali, Laure Lichon, Charlotte Cure, Stéphane Diring, Marwan Kobeissi, Fabrice Odobel, Magali Gary-Bobo

Journal of Photochemistry & Photobiology, B: Biology 253 (2024) 112863

Contents lists available at ScienceDirect

Journal of Photochemistry & Photobiology, B: Biology

journal homepage: www.elsevier.com/locate/jphotobiol

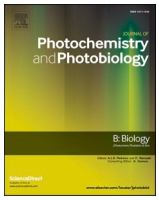

# Exceptional anticancer photodynamic properties of [1,4-Bis (3,6,9,12-Tetraoxatridec-1-yloxy)phthalocyaninato]zinc(II)

Christophe Nguyen [a,1], Isabelle Toubia [b,1], Kamel Hadj-Kaddour [a], Lamiaa M.A. Ali [a,c], Laure Lichon [a], Charlotte Cure [a], Stéphane Diring [b], Marwan Kobeissi [d], Fabrice Odobel [b,*], Magali Gary-Bobo [a,*]

[a] IBMM, Univ Montpellier, CNRS, ENSCM, Montpellier, France
[b] Nantes Université, CNRS, CEISAM, UMR 6230, F-44000 Nantes, France
[c] Department of Biochemistry, Medical Research Institute, University of Alexandria, 21561 Alexandria, Egypt
[d] Laboratoire RammalRammal, Equipe de Synthèse Organique Appliquée SOA, Université Libanaise, Faculté des Sciences 5, Nabatieh, Lebanon

ARTICLE INFO

*Keywords:*
Zinc phthalocyanines
Photodynamic therapy
Breast cancer cells
Healthy fibroblasts

ABSTRACT

Phthalocyanines have been described as effective photosensitizers for photodynamic therapy and are therefore, being studied for their biomedical applications. The metalation of photosensitizers can improve their photodynamic therapy potential. Here, we focus on the biological properties of [1,4-Bis(3,6,9,12-Tetraoxatridec-1-yloxy) phthalocyaninato]zinc(II) (ZnPc($\alpha EG_4$)$_2$) and demonstrate its exceptional anticancer activity upon light stimulation to kill preferentially cancer cells with a start of efficiency at 10 pM. Indeed, in this work we highlighted the high selectivity of ZnPc($\alpha EG_4$)$_2$ for cancer cells compared with healthy ones and we establish its mechanism of action, enabling us to conclude that ZnPc($\alpha EG_4$)$_2$ could be a powerful tool for cancer therapy.

## 1. Introduction

In the race against cancer, focused therapies gained a high place in the therapeutic arsenal due to their selective anticancer efficiency with few side effects. Photodynamic therapy (PDT) is rapidly developing as focused cancer treatment, evidenced by the numerous on-going clinical trials [1–4]. In principle, all visible wavelengths can be used in PDT to excite photosensitizers, but working in the phototherapeutic window constituted by red or near infrared wavelengths is more biocompatible since it allows a higher penetration depth in biological tissues [5–10], and avoids the excitation of endogenous chromophores such as hemoglobin or melanin [11].

Phthalocyanines are highly potent and attractive photosensitizers (PSs), thanks to their maximum absorption centered at 700 nm. They are also very efficient for PDT due to their ability to generate singlet oxygen when excited in the red visible region around 700 nm. In addition, their biomedical potential could be increased by metalation and introduction of substituents on phthalocyanine macrocycle as it enables to tune the solubility and the electronic properties such as fluorescence emission and generation of reactive oxygen species [12–19]. The [1,4-Bis (3,6,9,12-Tetraoxatridec-1-yloxy)phthalocyaninato]zinc(II) ZnPc ($\alpha EG_4$)$_2$ was earlier reported by Liu and co-workers [20,21] and its PDT activity was investigated on HT29 and HepG2 cancer cell showing certain efficiency with half maximal inhibitory concentration ($IC_{50}$) of 0.13 μM and 0.06 μM, respectively. Amphiphilic ZnPc($\alpha EG_4$)$_2$ presented in Scheme 1, is characterized by low tendency to aggregate in solution, quite red shifted absorption band located around 700 nm and good singlet oxygen generation featuring attractive key properties for PDT.

In this work, we have studied in more details the biological properties of ZnPc($\alpha EG_4$)$_2$ on MCF-7 cancer cell line and on healthy fibroblasts in order to determine if this compound could be a therapeutic tool for cancer cells targeting while preserving healthy cells. The present study reveals the exceptional anticancer activity of ZnPc($\alpha EG_4$)$_2$ ($LC_{50}$ = 1 nM on MCF-7) under light stimulation, its high selectivity, its very rapid internalization, its action on the cell cycle and particularly by increasing the S phase and finally its biocompatibility thanks to its low toxicity in the darkness and daylight on healthy cells making it an appealing drug for clinical applications and a strong molecular basement to design other PDT related sensitizers.

* Corresponding authors.
*E-mail addresses:* mkobeissi@ul.edu.lb (M. Kobeissi), Fabrice.Odobel@univ-nantes.fr (F. Odobel), magali.gary-bobo@inserm.fr (M. Gary-Bobo).
[1] These authors contributed equally to this study.

https://doi.org/10.1016/j.jphotobiol.2024.112863
Received 18 November 2023; Received in revised form 18 January 2024; Accepted 5 February 2024
Available online 6 February 2024

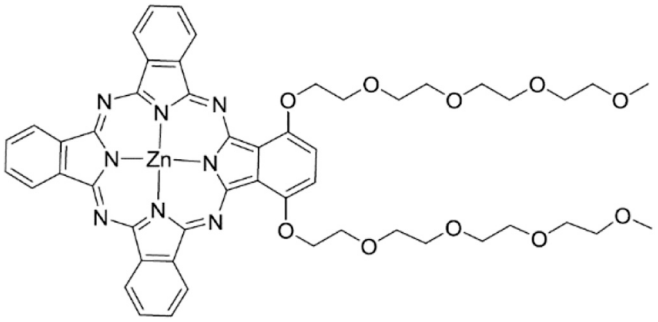

**Scheme 1.** Structures of the ZnPc($\alpha EG_4$)$_2$ investigated in this study.

## 2. Experimental Part

ZnPc($\alpha EG_4$)$_2$ was synthesized as previously published [20,21].

### 2.1. Cell Culture

Human breast adenocarcinoma cell line (MCF-7) and human dermal fibroblasts (FC-0024) were purchased from ATCC. MCF-7 cells were cultured in Dulbecco Eagle's Minimal Essential Medium/Ham's Nutrient Mixture F-12 (DMEM/F-12) supplemented with 10% fetal bovine serum (FBS) and 1% penicillin/streptomycin (P/S). Fibroblasts were maintained in Roswell Park Memorial Institute (RPMI) medium supplemented with 10% FBS and 1% P/S. Both cell lines were allowed to grow in humidified atmosphere at 37 °C under 5% $CO_2$.

### 2.2. Cytotoxicity Study

Cells were seeded into 96-well plates at a density of 1000 cells *per* well. Before incubating the compound with cells, and in order to minimize the risk of precipitation due to solubilization of compound in aqueous media, ZnPc($\alpha EG_4$)$_2$ was first dissolved in EtOH at an initial concentration of 10 mM (vortex and ultrasound bath), then cascaded in 10-fold dilutions in culture media. This strategy allows us to control the absence of precipitation for an optimal biodisponibility. One day after, cells were incubated with or without different concentrations of ZnPc ($\alpha EG_4$)$_2$ (from 0.001 to 100 μM) for 72 h in the dark. To quantify the percentage of living cells, cells were incubated 4 h with 0.5 mg.mL$^{-1}$ MTT (3-(4, 5-dimethylthiazol-2-yl)-2,5-diphenyltetrazoliumbromide) a colorimetric assay related to mitochondrial enzyme activity. The MTT/media solution was then removed and the precipitated crystals were dissolved in ethanol/DMSO (*v*/v). The solution absorbance was read at 540 nm using microplate reader.

### 2.3. Phototoxicity Study

MCF-7 cells were seeded into 96-well plates at a density of 1000 cells *per* well and allowed to grow for 24 h. Then, cells were incubated at different times, with or without increasing concentrations of ZnPc ($\alpha EG_4$)$_2$. Control cells were incubated with equivalent volumes of vehicle. After incubation, cells were submitted or not to laser irradiation (650 nm, 20 min, 39 J.cm$^{-2}$). Two days after irradiation, MTT assay was performed to quantify the level of living cells.

### 2.4. Statistical Analysis

Student's *t*-test was performed to compare paired groups of data. A $p$ value $<0.05$ was considered as statistically significant.

### 2.5. Cell Cycle Analysis

The cell cycle distribution was monitored by flow cytometry analysis. MCF-7 cells were seeded in 6-well plate and allowed to grow for 24 h. Cells were then treated with 100 nM of ZnPc($\alpha EG_4$)$_2$ for 1, 24 or 72 h. After treatment cells were harvested. Subsequently, 900 μL of an ice-cold hypotonic staining solution (25 μg.mL$^{-1}$ propidium iodide, 0.1% (*w/v*) tri-sodium citrate dihydrate, 10% (*v*/v) RNase A solution and 0.1% (v/v) Triton X-100 in distilled water), was added. Cells were kept overnight on ice and analysed for DNA content by a Gallios 10 photomultiplicators (Beckmancoulter) in Montpellier Rio Imaging facilities (MRI platform, Montpellier, France). The cell cycle distribution was analysed using KALUZA flow analysis software (Beckmancoulter). For each experiment, 20 000 events *per* sample were recorded.

### 2.6. Annexin V Expression Detection

MCF-7 cells were seeded on cover slips and allowed to grow for 24 h. Then, they were incubated with or without ZnPc($\alpha EG_4$)$_2$ at 100 nM concentration for 3 h in the dark or under laser excitation (650 nm, 20

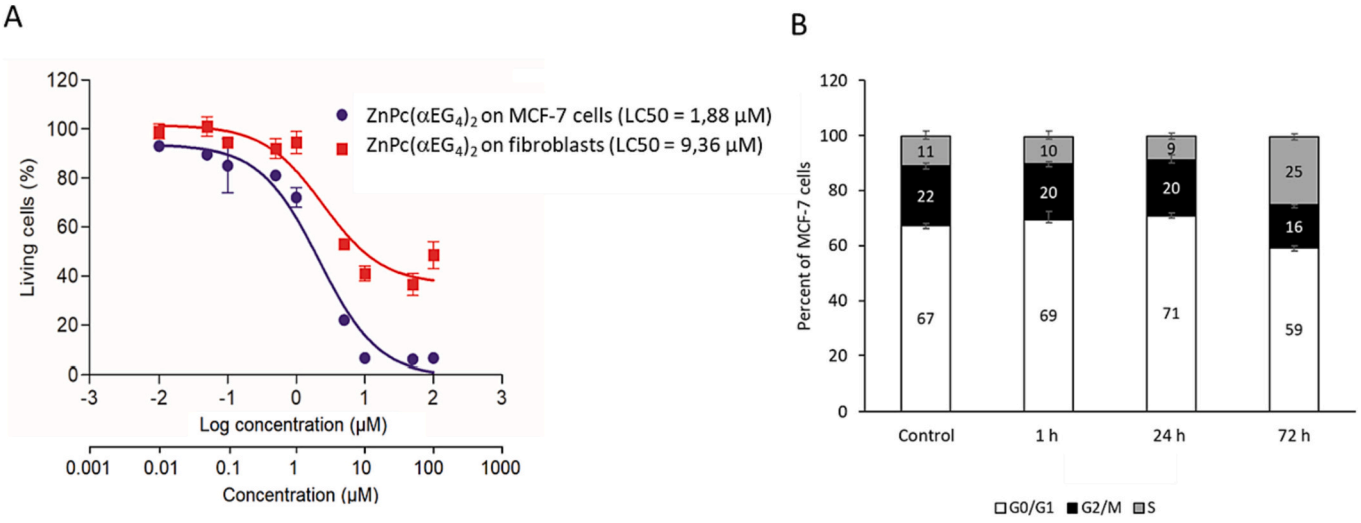


**Fig. 1.** ZnPc($\alpha EG_4$)$_2$ effect on cancer and healthy cells. (A) Cytotoxicity analysis of MCF-7 cells and healthy fibroblasts incubated for 72 h with increasing concentrations of ZnPc($\alpha EG_4$)$_2$ (from 1 nM to 100 μM). Living cell quantification was performed by MTT assay. Values reported are means ± standard deviations of 3 experiments. (B). Cell cycle analysis of MCF-7 cells incubated for 1, 24 or 72 h with 100 nM of ZnPc($\alpha EG_4$)$_2$. Flow cytometry study was performed to quantify cells in different cycle phases. Values are means ± standard deviations of 2 experiments.

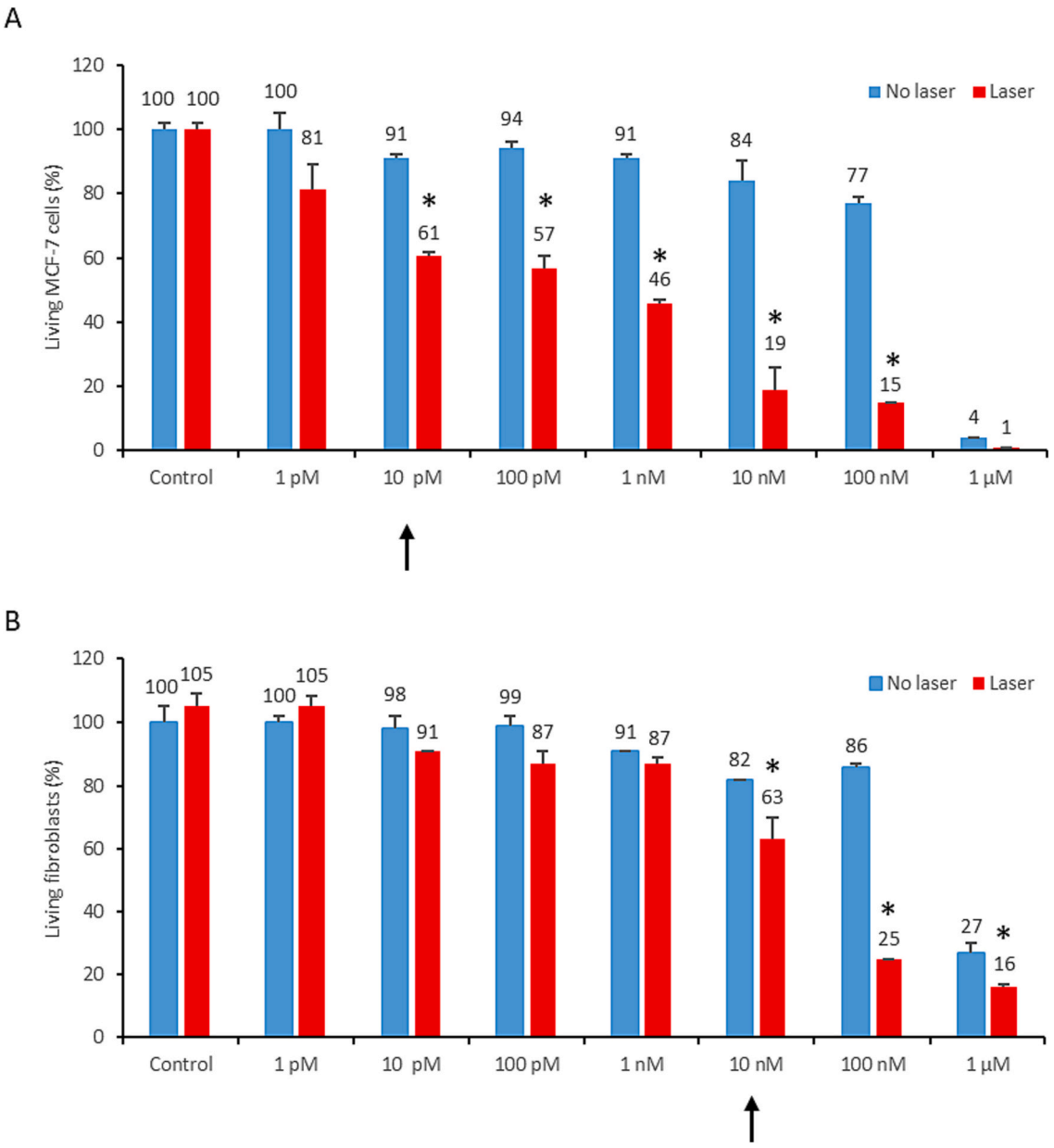


**Fig. 2.** PDT efficiency of ZnPc(αEG$_4$)$_2$ on cancer and healthy cells. (A) MCF-7 cells (B) or healthy fibroblasts were incubated for 24 h with increasing concentrations of ZnPc(αEG$_4$)$_2$ (from 1 pM to 1 µM). Light irradiation was performed with a red laser (λexc = 650 nm, 20 min, 39 J.cm$^{-2}$). Living cell quantification was performed 48 h after irradiation by MTT assay. Values are means ± standard deviations of 3 experiments. * $p < 0.05$, significantly different from No laser. The arrows point to the concentration of ZnPc(αEG$_4$)$_2$ for which the PDT effect becomes significant. (For interpretation of the references to colour in this figure legend, the reader is referred to the web version of this article.)

min, 39 J.cm$^{-2}$). Cells were incubated with 5 µL of annexin V-FITC (from abcam) for 5 min, in darkness and at room temperature. Then, cells were rinsed twice and imaged under fluorescent microscope Leica DM IRB.

### 2.7. Reactive Oxygen Species (ROS) Production

MCF-7 cells were incubated with 100 nM of ZnPc(αEG$_4$)$_2$ for 24 h and submitted or not to laser excitation (650 nm, 20 min, 39 J.cm$^{-2}$). However, 45 min before excitation, cells were incubated with 20 µM of 2′,7′ –dichlorofluorescin diacetate (DCFDA / H$_2$DCFDA-Cellular ROS Assay Kit-ab113851). After excitation, cells were washed with cell media and fluorescence emission of 2′, 7′ –dichlorofluorescein (DCF) ($\lambda_{exc}$ = 480 nm) was collected using the camera of standard fluorescence microscope.

## 3. Results and Discussion

The cytotoxicity induced by the exposition of human cells to increasing concentrations of ZnPc(αEG$_4$)$_2$ was studied. In the experiment presented in Fig. 1A, human cancer and healthy cells (MCF-7 cells and fibroblasts, respectively) were incubated for 3 days with ZnPc (αEG$_4$)$_2$. The concentration range was chosen between 1 nM and 100 µM in order to determine the 50% of the lethal concentration (LC$_{50}$). The quantification of living cells after 3 days was obtained by a colorimetric assay (MTT) and the obtained results demonstrated that breast cancer cells (MCF-7) are strongly more sensitive to ZnPc(αEG$_4$)$_2$ than healthy fibroblasts. In the dark, the LC$_{50}$ values of MCF-7 cells and fibroblasts are 1.88 ± 0.09 µM and 9.36 ± 0.56 µM, respectively, showing that this compound is around 5 fold more toxic on cancer cells than healthy ones (Fig. 1A). Another advantage of ZnPc(αEG$_4$)$_2$ against cancer cells could

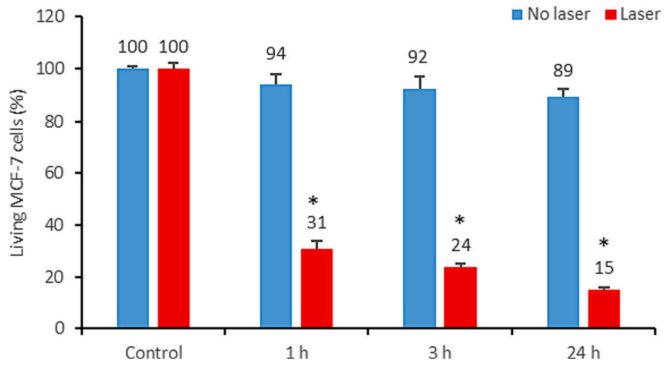


**Fig. 3.** Kinectic study of PDT efficiency of ZnPc($\alpha EG_4$)$_2$ on cancer cells. MCF-7 cells were incubated for 1, 3 or 24 h with ZnPc($\alpha EG_4$)$_2$ at 100 nM. Light irradiation was performed with a red laser ($\lambda$exc = 650 nm, 20 min, 39 J.cm$^{-2}$). Living cell quantification was performed 48 h after irradiation by MTT assay. Values are means ± standard deviations of 3 experiments. * $p < 0.05$, significantly different from No laser. (For interpretation of the references to colour in this figure legend, the reader is referred to the web version of this article.)

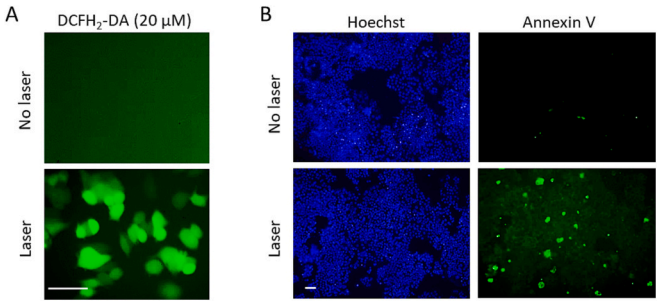


**Fig. 4.** ROS production and annexin V expression. (A) Demonstration of ROS production in MCF-7 cells incubated for 24 h with 100 nM of ZnPc($\alpha EG_4$)$_2$, then incubated with DCFH$_2$-DA (20 µM, 45 min) and irradiated for 20 min at 650 nm. The green fluorescence inside the cells reflects ROS production (imaged at 480 nm). (B) Annexin V-FITC staining for apoptosis markers detection after 3 h incubation time with 100 nM of ZnPc($\alpha EG_4$)$_2$ and submitted or not to laser irradiation. Nuclei of cells were stained by Hoechst 33342. Scale bar: 20 µm. (For interpretation of the references to colour in this figure legend, the reader is referred to the web version of this article.)

be due to its action on cell cycle phases. Indeed, it has already been described that anticancer molecules can cause cell cycle arrest and lead to apoptosis of cancer cells [22]. For this purpose, we have studied the effect of MCF-7 cells incubation with 100 nM of ZnPc($\alpha EG_4$)$_2$ for 1, 24 or 72 h and we have observed an increase in S phase after 72 h of treatment suggesting a blocking of cells in this state (Fig. 1B). This cell cycle blockade could have several origins and may be due to a modification of the cell cycle regulators such as cyclins, or DNA damage such as DNA methylation [23–25].

Then, the PDT effect in cancer and healthy cells was studied. For this objective, PDT experiments were performed at 650 nm and at various concentrations of ZnPc($\alpha EG_4$)$_2$ incubated for 24 h with MCF-7 cells or fibroblasts (Fig. 2). The experiments were performed with concentrations range from 1 pM to 1 µM and the resulting PDT effect was tremendous. Although JY Liu et al., had already described a PDT effect on human cancer colorectal (HT29) or hepatic (HepG2) cells [21], and even if this effect was very good (with nanomolar efficiency in the best conditions) this was not in the same proportions as that measured in this study. Indeed, in our experiments, 48 h after the irradiation of MCF-7 cells treated with ZnPc($\alpha EG_4$)$_2$ we noticed a significant effect from 10 pM that is an exceptional efficiency. This effect increases depending on the concentration to reach 50% cell death at 1 nM, under laser excitation at 650 nm for 20 min (39 J.cm$^{-2}$). These last data are approximately in correlation with the study of JY Liu and coworkers. The difference between their work and ours is that, in their paper, the most effective PDT was obtained for a few tens of nM on the HT29 and HepG2 cancer lines while we obtained an efficiency 10 or 100 times greater on MCF-7 cells. Interestingly, this strong effect on cancer cells was never observed in healthy cells. As shown by the black arrows on Fig. 2, a significant effect of PDT on MCF-7 cells incubated with 10 pM of ZnPc($\alpha EG_4$)$_2$ can be observed with 30% cell death, while the PDT effect becomes significant on healthy fibroblasts from 10 nM with 19% cell death. This is a crucial point, indeed, in a previous work [30] we have studied the PDT effect of ZnPc($\beta EG_3$)$_4$ and showed that this compound was as phototoxic in MCF-7 cells as in healthy fibroblasts. Here, the difference of activity between cancer and healthy cells is very interesting and suggests a biomedical application for ZnPc($\alpha EG_4$)$_2$ in the treatment of cancer by PDT without generating too many side effects on healthy tissues.

For a better understanding of ZnPc($\alpha EG_4$)$_2$ PDT efficiency, a kinetic study of this compound at 100 nM was performed. The results, presented in Fig. 3, show that this compound exhibits a time dependent activity with a very strong effect even after short incubation times followed by laser excitation (only 31% living cells after 1 h incubation).

This early efficiency suggests a very quick internalization of this compound in cancer cells, which is an important parameter for its potential medical application.

We confirmed the PDT mechanism by demonstrating the ROS production during the laser excitation (Fig. 4A) and also the activation of apoptotic pathway by detecting apoptosis markers such as Annexin V (Fig. 4B).

Firstly, ROS production was studied and the results are shown in Fig. 4A. For this, cells were incubated with DCFH$_2$-DA (2′,7′ -dichlorodihydrofluorescein diacetate), a non-fluorescent molecule. In the presence of ROS this molecule is oxidized into the fluorescent 2′,7′ -dichlorodihydrofluorescein (DCF), whose green luminescence was detected using a fluorescence microscope. The results show that in the presence of 100 nM of ZnPc($\alpha EG_4$)$_2$, light excitation induced green fluorescence inside the cancer cells incubated 24 h with ZnPc($\alpha EG_4$)$_2$. This demonstrates ROS production and confirms that the cell death was generated by PDT induced mechanism [26]. In accordance with this result, the expression of annexin V [27] was also increased in cancer cells incubated for 3 h with 100 nM of ZnPc($\alpha EG_4$)$_2$ and excited with laser (Fig. 4B). Since annexin V is a marker of early apoptosis, this obtained result supports the hypothesis that the induced cell death is apoptosis, as described for PDT.

We have already demonstrated the biomedical potential of ZnPc ($\alpha EG_4$)$_2$ thanks to the stronger PDT efficiency on cancer cells than healthy ones. In order to demonstrate further its applicability, the effect of such treatment was also explored when the cells were simply exposed to daylight. Indeed, we can suppose that the compound will react to the ambient light. As shown in Fig. 1, describing an experiment for which the plate was totally maintained in the darkness during all the time of the experiment, the cell death was about 20% and 50% for fibroblasts and MCF-7 respectively. In Fig. 2, an experiment for which the plate was punctually exposed to the ambient light, the cell death was high. However, it is important that the PS presents a specificity in the activating wavelength in order to induce better control of the therapeutic conditions. Therefore, we have incubated cancer and healthy cells with increasing concentrations of ZnPc($\alpha EG_4$)$_2$ and exposed them to darkness or daylight during 4 h. Two days after exposition to daylight (or not) the viability of cells was quantified and reported in Fig. 5A and B. It can be observed that cancer cells become significantly more sensitive to daylight at 100 nM while healthy cells are not impacted at all before 1 µM. This confirms the compatibility of ZnPc($\alpha EG_4$)$_2$ treatment for clinical applications.

## 4. Conclusion

In this study, we have demonstrated that ZnPc($\alpha EG_4$)$_2$ exhibited a

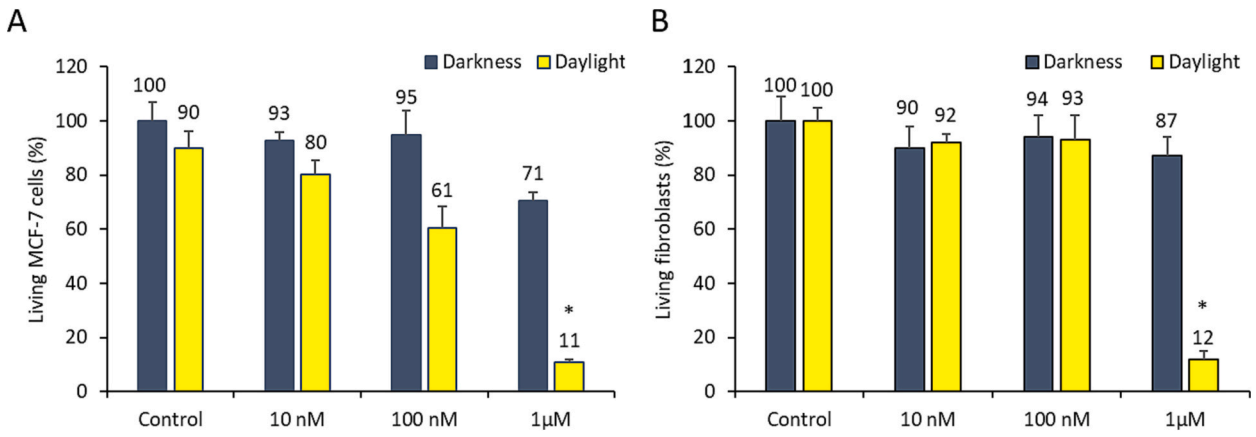


**Fig. 5.** Study of daylight effect on ZnPc$(\alpha EG_4)_2$ treated cells. (A) MCF-7 cells and (B) fibroblasts were incubated 24 h with ZnPc$(\alpha EG_4)_2$ at 10 nM, 100 nM or 1 µM and exposed or not (Darkness) for 4 h to daylight. Living cell quantification was performed 48 h after irradiation by MTT assay. Values are means ± standard deviations of 3 experiments. * $p < 0.05$, significantly different from Darkness.

better cytotoxic effect on cancer cells with $LC_{50}$ 5 folds higher in healthy cells than in cancer ones. This effect is probably due at least in part to a modification in the cell cycle with a S phase arrest of cancer cells. In addition, the PDT great potential was highlighted with a significant effect under laser excitation at 650 nm for 10 pM on cancer cells. Importantly, this phototoxicity appears only at 10 nM for healthy cells. This strong discrimination between healthy and cancer cells is a crucial advantage for a medical use where we could imagine to kill cancer cells with a dose that has no effect on healthy cells. In addition, with higher concentrations, this PDT effect could be obtained after only 1 h incubation time. Finally, it is important to note that the daylight does not activate ZnPc$(\alpha EG_4)_2$ in healthy cells in the conditions of PDT efficiency.

All together, these data described the tremendous PDT effect of ZnPc $(\alpha EG_4)_2$ and its important selectivity on cancer cells, compared to other glycosylated ZnPc [30], suggesting a possible biomedical efficiency with low side effects on healthy cells and fewer constraints of staying in the dark during the first weeks of treatment. In a forthcoming study, we could envisage the design of a covalent dyad based on this zinc phthalocyanine and combined with a chemotherapeutics agent and hoping to obtain a synergistic effect between the two entities to increase the delivery of this chemotherapy to the cancer cells and benefit at the same time from the PDT effect [28–30].

## CRediT authorship contribution statement

**Christophe Nguyen:** Methodology, Investigation, Conceptualization. **Isabelle Toubia:** Investigation, Conceptualization. **Kamel Hadj-Kaddour:** Investigation. **Lamiaa M.A. Ali:** Investigation, Conceptualization. **Laure Lichon:** Investigation. **Charlotte Cure:** Investigation. **Stéphane Diring:** Investigation. **Marwan Kobeissi:** Supervision, Conceptualization. **Fabrice Odobel:** Writing – original draft, Supervision, Conceptualization. **Magali Gary-Bobo:** Writing – original draft, Conceptualization.

## Declaration of competing interest

The authors declare that they have no known competing financial interests or personal relationships that could have appeared to influence the work reported in this paper.

## Data availability

Data will be made available on request.

## References

[1] P. De Silva, M.A. Saad, H.C. Thomsen, S. Bano, S. Ashraf, T. Hasan, Photodynamic therapy, priming and optical imaging: potential co-conspirators in treatment design and optimization — a Thomas Dougherty award for excellence in PDT paper, J. Porphyrins Phthalocyanines 24 (11n12) (2020) 1320–1360, https://doi.org/10.1142/S1088424620300098.

[2] C. Frochot, S. Mordon, Update of the situation of clinical photodynamic therapy in Europe in the 2003–2018 period, J. Porphyrins Phthalocyanines 23 (04n05) (2019) 347–357, https://doi.org/10.1142/S1088424619300027.

[3] H.O. Alsaab, M.S. Alghamdi, A.S. Alotaibi, R. Alzhrani, F. Alwuthaynani, Y. S. Althobaiti, A.H. Almalki, S. Sau, A.K. Iyer, Progress in clinical trials of photodynamic therapy for solid tumors and the role of nanomedicine, Cancers 12 (10) (2020) 2793, https://doi.org/10.3390/cancers12102793.

[4] A. Kawczyk-Krupka, A.M. Bugaj, W. Latos, K. Zaremba, K. Wawrzyniec, A. Sieroń, Photodynamic therapy in colorectal cancer treatment: the state of the art in clinical trials, Photodiagnosis Photodyn. Ther. 12 (3) (2015) 545–553, https://doi.org/10.1016/j.pdpdt.2015.04.004.

[5] W. Fan, B. Yung, P. Huang, X. Chen, Nanotechnology for multimodal synergistic cancer therapy, Chem. Rev. 117 (22) (2017) 13566–13638, https://doi.org/10.1021/acs.chemrev.7b00258.

[6] J. Sun, E. Feng, Y. Shao, F. Lv, Y. Wu, J. Tian, H. Sun, F. Song, A selenium-substituted heptamethine cyanine photosensitizer for near-infrared photodynamic therapy, ChemBioChem 23 (2022) e202200421, https://doi.org/10.1002/cbic.202200421.

[7] S. Veeranarayanan, M.S. Mohamed, A.C. Poulose, M. Rinya, Y. Sakamoto, T. Maekawa, D.S. Kumar, Photodynamic therapy at ultra-low NIR laser power and X-ray imaging using cu $_3$ BiS $_3$ nanocrystals, Theranostics 8 (19) (2018) 5231–5245, https://doi.org/10.7150/thno.25286.

[8] J. Zheng, Y. Liu, F. Song, L. Jiao, Y. Wu, X. Peng, A nitroreductase-activatable near-infrared theranostic photosensitizer for photodynamic therapy under mild hypoxia, Chem. Commun. (2020), https://doi.org/10.1039/D0CC02019B, 10.1039. D0CC02019B.

[9] F. Xu, H. Li, Q. Yao, H. Ge, J. Fan, W. Sun, J. Wang, X. Peng, Hypoxia-activated NIR photosensitizer anchoring in the mitochondria for photodynamic therapy, Chem. Sci. 10 (45) (2019) 10586–10594, https://doi.org/10.1039/C9SC03355F.

[10] P. Chinna Ayya Swamy, G. Sivaraman, R.N. Priyanka, S.O. Raja, K. Ponnuvel, J. Shanmugpriya, A. Gulyani, Near infrared (NIR) absorbing dyes as promising photosensitizer for photo dynamic therapy, Coord. Chem. Rev. 411 (2020) 213233, https://doi.org/10.1016/j.ccr.2020.213233.

[11] M. Wainwright, Therapeutic applications of near-infrared dyes, Color. Technol. 126 (2010) 115–126, https://doi.org/10.1111/j.1478-4408.2010.00244.x.

[12] P.-C. Lo, M.S. Rodríguez-Morgade, R.K. Pandey, D.K.P. Ng, T. Torres, F. Dumoulin, The unique features and promises of phthalocyanines as advanced photosensitisers for photodynamic therapy of cancer, Chem. Soc. Rev. 49 (4) (2020) 1041–1056, https://doi.org/10.1039/C9CS00129H.

[13] R.C.H. Wong, P.-C. Lo, D.K.P. Ng, Stimuli responsive phthalocyanine-based fluorescent probes and photosensitizers, Coord. Chem. Rev. 379 (2019) 30–46, https://doi.org/10.1016/j.ccr.2017.10.006.

[14] V. Abdul Rinshad, J. Sahoo, M. Venkateswarulu, N. Hickey, M. De, P. Sarathi Mukherjee, Solvent induced conversion of a self-assembled gyrobifastigium to a barrel and encapsulation of zinc-phthalocyanine within the barrel for enhanced photodynamic therapy, Angew. Chem. (2023) 135, https://doi.org/10.1002/anie.202218226.

[15] Ş. Doğan, M. Ince, F. Sogutlu, C.B. Avci, D. Özel, F. Yurt, Photodynamic therapy potential of cobalt phthalocyanine in triple-negative breast cancer, Polyhedron 245 (2023) 116617, https://doi.org/10.1016/j.poly.2023.116617.

[16] V. Mantareva, I. Iliev, I. Sulikovska, M. Durmuş, I. Angelov, Cobalamin (vitamin B12) in anticancer photodynamic therapy with Zn(II) Phthalocyanines, IJMS 24 (5) (2023) 4400, https://doi.org/10.3390/ijms24054400.
[17] N. Nwahara, G. Abrahams, J. Mack, E. Prinsloo, T. Nyokong, A hypoxia responsive silicon phthalocyanine containing naphthquinone axial ligands for photodynamic therapy activity, J. Inorg. Biochem. 239 (2023) 112078, https://doi.org/10.1016/j.jinorgbio.2022.112078.
[18] D. Liu, L. Jiang, J. Chen, Z. Chen, C. Yuan, D. Lin, M. Huang, Monomer and oligomer transition of zinc phthalocyanine is key for photobleaching in photodynamic therapy, Molecules 28 (12) (2023) 4639, https://doi.org/10.3390/molecules28124639.
[19] P. Balcik-Ercin, G. Ekineker, N. Salik, B. Aydoğdu, T. Yagci, M. Göksel, Arginine mediated photodynamic therapy with silicon(IV) phthalocyanine photosensitizers, Photodiagnosis Photodyn. Ther. 43 (2023) 103667, https://doi.org/10.1016/j.pdpdt.2023.103667.
[20] J.-Y. Liu, X.-J. Jiang, W.-P. Fong, D.K.P. Ng, Highly photocytotoxic 1,4-dipegylated zinc(ii) phthalocyanines. Effects of the chain length on the in vitro photodynamic activities, Org. Biomol. Chem. 6 (24) (2008) 4560, https://doi.org/10.1039/b814627f.
[21] J.-Y. Liu, P.-C. Lo, X.-J. Jiang, W.-P. Fong, D.K.P. Ng, Synthesis and in vitro photodynamic activities of Di-α-substituted zinc(ii) Phthalocyanine derivatives, Dalton Trans. No. 21 (2009) 4129, https://doi.org/10.1039/b817940a.
[22] K. Moloudi, H. Abrahamse, B.P. George, Photodynamic therapy induced cell cycle arrest and cancer cell synchronization: review, Front. Oncol. 13 (2023) 1225694, https://doi.org/10.3389/fonc.2023.1225694.
[23] G. Guha, W. Lu, S. Li, X. Liang, M.F. Kulesz-Martin, T. Mahmud, A.K. Indra, G. Ganguli-Indra, Novel pactamycin analogs induce P53 dependent cell-cycle arrest at S-phase in human head and neck squamous cell carcinoma (HNSCC) cells, PloS One 10 (5) (2015) e0125322, https://doi.org/10.1371/journal.pone.0125322.
[24] P. Doan, A. Musa, N.R. Candeias, F. Emmert-Streib, O. Yli-Harja, M. Kandhavelu, Alkylaminophenol induces G1/S phase cell cycle arrest in glioblastoma cells through P53 and cyclin-dependent kinase signaling pathway, Front. Pharmacol. 10 (2019) 330, https://doi.org/10.3389/fphar.2019.00330.
[25] H. Zhu, L. Zhang, S. Wu, F. Teraishi, J.J. Davis, D. Jacob, B. Fang, Induction of S-phase arrest and P21 overexpression by a small molecule 2[[3-(2,3-dichlorophenoxy)propyl] amino]ethanol in correlation with activation of ERK, Oncogene 23 (29) (2004) 4984–4992, https://doi.org/10.1038/sj.onc.1207645.
[26] L. Ming, K. Cheng, Y. Chen, R. Yang, D. Chen, Enhancement of tumor lethality of ROS in photodynamic therapy, Cancer Med. 10 (1) (2021) 257–268, https://doi.org/10.1002/cam4.3592.
[27] L.C. Crowley, B.J. Marfell, A.P. Scott, N.J. Waterhouse, Quantitation of apoptosis and necrosis by annexin v binding, propidium iodide uptake, and flow cytometry, Cold Spring Harb Protoc vol. 11 (2016), https://doi.org/10.1101/pdb.prot087288 pdb.prot087288.
[28] C. Lottner, K.-C. Bart, G. Bernhardt, H. Brunner, Hematoporphyrin-derived soluble porphyrin−platinum conjugates with combined cytotoxic and phototoxic antitumor activity, J. Med. Chem. 45 (10) (2002) 2064–2078, https://doi.org/10.1021/jm0110688.
[29] F. Schmitt, P. Govindaswamy, O. Zava, G. Süss-Fink, L. Juillerat-Jeanneret, B. Therrien, Combined arene ruthenium porphyrins as chemotherapeutics and photosensitizers for cancer therapy, J. Biol. Inorg. Chem. 14 (1) (2009) 101–109, https://doi.org/10.1007/s00775-008-0427-y.
[30] I. Toubia, C. Nguyen, S. Diring, M. Pays, E. Mattana, P. Arnoux, C. Frochot, M. Gary-Bobo, M. Kobeissi, F. Odobel, Study of cytotoxic and photodynamic activities of dyads composed of a zinc phthalocyanine appended to an organotin, Pharmaceuticals 14 (5) (2021) 413, https://doi.org/10.3390/ph14050413.